Published in final edited form as:
Semin Radiat Oncol. 2011 April ; 21(2): 147–156. doi:10.1016/j.semradonc.2010.11.001.

The Promise of Dynamic Contrast Enhance Imaging in Radiation Therapy

Yue Cao, Ph.D.
Departments of Radiation Oncology and Radiology, University of Michigan

Yue Cao: yuecao@umich.edu

Abstract

Dynamic contrast enhanced (DCE) magnetic resonance imaging (MRI) and computed tomography (CT) are emerging as valuable tools to quantitatively map the spatial distribution of vascular parameters such as perfusion, vascular permeability, blood volume, and mean transit time in tumors and normal organs. DCE MRI/CT have shown prognostic and predictive value for response of certain cancers to chemo and radiation therapy. DCE MRI/CT offer the promise of early assessment of tumor response to radiation therapy, opening a window for adaptively optimizing radiation therapy based upon functional alterations that occur earlier than morphological changes. DCE MRI/CT have also shown the potential of mapping dose-responses in normal organs and tissue for evaluation of individual sensitivity to radiation, providing additional opportunities to minimize risks of radiation injury. The evidence for potentially applying DCE MRI and CT for selection and delineation of radiation boost targets is growing. The clinical use of DCE MRI and CT as a biomarker or even a surrogate endpoint for radiation therapy assessment of tumor and normal organs must consider technical validation issues, including standardization, reproducibility, accuracy and robustness, as well as clinical validation of the sensitivity and specificity for each specific problem of interest. Although holding great promise, to date DCE MRI and CT have not been qualified as a surrogate endpoint for radiation therapy assessment or for treatment modification in any prospective phase III clinical trial for any tumor site.

Introduction

Molecular, functional and metabolic imaging methods have been developed and evaluated intensively as potential biomarkers for assessment of tumor response and outcome in radiation therapy, as well as for radiation target selection and delineation. The general investigational hypothesis is that biological imaging has superior sensitivity and specificity to tumor biological processes, and therefore can be utilized for better selection of radiation targets or for better indication of tumor early response to treatment as well as normal tissue injury.[1,2] These biological indications could provide additional information, either prognostic or predictive, beyond the conventional clinical factors.[3-5] A prognostic indicator can be employed to stratify patients for different treatment strategies, while a predictive indicator can be used for therapy modification, e.g., treatment intensification for non-

Yue Cao, Associate Professor, Department of radiation Oncology, University of Michigan, 400 W William St, Argus Building 1, Ann Arbor MI 48103

responsive tumors. Similarly, functional imaging has been used to assess individual variations in sensitivity to radiation-induced normal tissue toxicity, with the intent of applying these methods to adjust radiation doses to organs-at-risk.

Dynamic contrast enhanced (DCE) and dynamic susceptibility contrast (DSC) MRI and DCE CT have been developed and evaluated, to some extent, technically and pathophysiologically for characterization of vascular properties in the tumor and normal organ tissue.[6-14] Vascular properties derived from these imaging studies include blood volume, blood flow, vascular permeability, and mean transit time as well as distribution volume and available interstitial space for the contrast agent. Many malignant tumors manifest neovascularity or angiogenesis, a process of recruiting, synthesizing and forming new vascular networks, as a possible aspect of tumor growth, proliferation and metastasis.[10-12,15-20] As a result, these newly synthesized vessels manifest high permeability, tortuosity, and density heterogeneity as well as poor functionality. Therefore, vascular characteristics of a tumor could prove a prognostic indicator of its aggressiveness.[5,15,16,18] Also, vascular networks provide oxygen and nutrition supply to the tumor and normal tissue.

Without adequate blood and oxygen supply to tumor cells, effectiveness of radiation treatment of the tumor can be compromised. For example, a hypoxic tumor or tumor subvolume responds to radiation therapy poorly compared to a similarly treated cluster of normoxic tumor cells.[21-24] Perfusion characteristics of a tumor or tumor subvolume prior to RT as well as the subsequent alteration during the early course of treatment could provide guidance on where to intensify the treatment.[3,5,15,16,18,25,26] Recent developments in prognostic biomarkers, e.g., O6 methylguanine-DNA methyltransferase (MGMT) promoter methylation status for GBM treated by concomitant radiochemotherapy,[27] and human papillomavirus (HPV) for ororpharygeal cancer,[28,29] provide a means to differentiate certain classes of patients with favorable versus unfavorable outcome. However, imaging prognostic or predictive biomarkers could address where in the tumor as well as which tumor does not respond to RT. For instance, despite the improvements in treatment regimens for ororpharygeal cancer, there are still up to 20%-50% failure rates, including metastatic and locoregional failures, especially in patients who are smokers[30] and testing negative for HPV infection.[29,31] Combining these biological and imaging biomarkers could improve the predictive power for outcome. Furthermore, normal tissue vasculature is prone to radiation damage, which can result in injury of organ function and cause poor quality of life and even mortality in severe cases. Radiation-induced injury to normal tissue has presented as a limiting factor for high dose radiation therapy for certain body sites, e.g., liver, lung and brain. Monitoring tumor and normal tissue response to treatment during the early course of radiation therapy could allow us to better estimate a therapy index for individual patients, and modify the treatment strategy based upon the individual risk and benefit.

DCE imaging as a biomarker for prediction of tumor response and outcome to RT, as evidenced in brain, head and neck, and cervical cancers, will be discussed in this review. DCE imaging of normal tissue dose response as well as its role in prediction of organ toxicity are emerging, and will be discussed. Vascular features in the tumor or sub-volume of the tumor, delineated by quantitative analysis of DCE imaging, has been recognized to have the potential to define radiation boost volume. Limited pathological and clinical validation, particularly for radiation therapy specific changes, hinder the advancement of this class of imaging biomarkers for application in radiation therapy. DCE imaging still faces great challenges in technical standardization and validation, as well as in pathological and clinical validation, in order to qualify it as a surrogate endpoint for radiation therapy assessment and to utilize it for radiation target definition. These issues will be discussed.

Prognostic and predictive indicators for Tumor Response Assessment

Malignant gliomas, particularly GBM, exhibit neovascularity characterized as abnormally rapid growth of vasculature with high density, great vessel leakage, abnormal perfusion and prolonged mean transit time, which is possibly mediated by angiogenesis and has become the target of anti-angiogenic therapy.[32,33] Cerebral blood volume (CBV), cerebral blood flow (CBF) and vascular permeability in gliomas mapped by DCE or DSC MRI prior to radiation have been shown to be prognostic factors for treatment response and outcome.[4,5,15,16] The common and consistent finding from these studies is that a malignant glioma with high CBV, high CBF or high permeability is associated with poor response, short time to progression, or worse survival.

An early prospective study shows that for patients who have high-grade glioms with great fractional tumor volumes of high CBV survival is significantly worse than those who have small fractional tumor volumes with high CBV (Fig 1).[16] A retrospective study with a large series of 189 patients with low- or high-grade glioma shows that relative tumor CBV before RT predicts time to progression after therapy better than the pathological grade.[5] For tumors with high relative CBV (>1.75) prior to radiation treatment (RT), irrespective of pathological grades, the median of time to progression was found to be 8.8 months; whereas for tumors with low relative CBV (<1.75) before RT, there was a significant difference in time to progression between patients with low and high grade gliomas. Another study showed that a large sub-volume of the tumor with high vascular permeability in patients with high grade gliomas prior to RT was associated with worse survival, whereas the tumor volume defined by FLAIR abnormality, post-Gd T1 image, or contrast-enhanced rim was not.[15] Mapping the glioma CBV and vascular permeability prior to RT could aid in identifying patients at risk for poor outcome for treatment intensification by either radiation or combining radiation with chemo and/or targeted therapy.

Re-assessment of treatment strategies during the early course of RT can provide a feedback measure allowing for re-adjustment of individual therapy. Evaluation of the response rate of glioma CBV and CBF during the mid-course of fractionated RT may be valuable for identifying non-responders from responders. Several studies of malignant gliomas have shown that changes in tumor CBV and CBF after 3 weeks of the 6-week course of RT to be predicative for outcome,[16,34] and differentiate pseudo-progression from progression.[35]

In addition to assessing overall tumor response to RT, identifying the sub-volume of the tumor resistant to therapy during the course of treatment can have substantial implication in selection and delineation of radiation boost targets. This requires development and validation of quantitative analysis methodologies to differentiate tumor responsive sub-volumes from non-responsive ones, and their association with patterns of failure and outcome. These heterogeneous responses are possibly due to tumor heterogeneity, which can be targeted by local therapy like radiation. Utilization of CBV and CBF for target definition of malignant gliomas in radiation therapy requires further validation, including by pathophysiology and/or tumor pattern failure analyses. Finally, alteration of response pattern of CBV and CBF in gliomas treated by concurrent RT and targeted therapy, e.g., anti-angiogenesis drugs,[33] requires studies to re-establish these biomarkers under altered therapeutic conditions.

The predictive value of quantitative CBF and CBV imaging for response assessment has also been demonstrated in patients who have brain metastases and are treated with stereotactic radiosurgery (SRS).[36,37] Although pre-SRS regional CBV and CBF failed to predict therapy outcome in these studies, perfusion imaging at 6-week follow-up shows high sensitivity and specificity for treatment outcome prediction. A decrease in tumor CBV 6

weeks after SRS has 91% sensitivity and 71% specificity for prediction of treatment outcome determined 5 months later, which is superior to the 64% sensitivity and 43% specificity of morphological changes in tumor volume evaluated at the same time.[36] It seems that functional and physiological changes of tumor tissue after irradiation occur earlier than morphological changes. Although pseudo-progression is less pronounced in brain metastases treated by SRS than GBM treated by chemoradiation therapy,[38] changes in regional CBV and CBF during follow-up evaluation as early as 6 weeks may help in distinguishing the extent of response, thus potentially supporting earlier adjuvant treatment decisions.

Hypoxia has significant implications for the effectiveness of radiation therapy. Certain tumors have been long recognized to have a high probability to be hypoxic(e.g., cervical and head and neck cancers). It is reasonable to assume that low blood flow and low blood volume in cervical tumors or a sub-volume of such tumors can indicate a patient who is prone to fail conventional radiation treatment. This hypothesis has motivated several studies to investigate the prognostic value of dynamic contrast enhancement patterns on MRI in cervical cancer patients prior to radiation therapy.[39-42] The sub-volume of a cervical tumor with poor contrast enhancement is identified clinically as a predictor for local failure, which is independent of the tumor volume. Interestingly, a histopathological study shows that the well-enhanced sub-volumes are predominantly composed of cancer cell fascicles, whereas poorly enhanced areas are composed of fibrous tissue with scattered cancer cells.[42] Nevertheless, radiation therapy is more effective for the well perfused tumor cells than poorly perfused ones.[42]

A recent study further investigated the temporal changes of dynamic enhanced patterns in cervical cancer during the course of radiation therapy and their association with local control and survival.[43] This study confirmed the previous finding that better 5-year local control and survival rates are achieved in the patients who have no or small sub-volumes of tumors with poor enhancement than ones that have largely poorly enhanced subvolumes within the tumor. Most interestingly, if tumor poor enhancement improved during the early course of radiation therapy, the patients had tumor local control and survival better than those patients having poor enhancement persist to the mid-course of treatment. Although outcome was favorable in patients with initially high contrast enhanced cervical cancers, a longitudinal investigation of microenvironment changes in the tumor, e.g., perfusion and oxygenation, during the early course of RT could further guide individualized therapy.

Similar to cervical cancer, tumor oxygenation in the primary sites and metastatic lymph nodes of head and neck cancer has been recognized as a prognostic factor independent of other known clinical variables.[21-23] Non-invasive, in vivo mapping of oxygenation and perfusion of head and neck tumors has suggested its added value for prognosis of outcome. Recently, prognostic and predictive functional and metabolic imaging studies that assess tumor hypoxia or tumor perfusion prior to therapy in HNC have been described.[3,26,44-49] Interestingly, studies of the patients with HNC using dynamic 18F-fluoromisonidazole (FMISO) PET [49] or DCE MRI and F-MISO PET[50] have found that hypoxia and perfusion provided complementary information, an inverse correlation in the tumor, and the pattern of pre-RT tumor hypoxia or perfusion is correlated with outcomes of RT.

It appears that the parametric map derived from DCE imaging is able to detect the poorly perfused sub-tumor volume below the detectability of FMISO, as indicated in a study.[50] In a large series of a perfusion study of 105 patients with HNC treated by RT, low tumor perfusion prior to RT was associated with high local failure,[3] suggesting that poorly perfused HN tumors respond poorly to RT. Furthermore, pre-therapy tumor perfusion has been identified as an independent predictor of T-stage classification for local failures. Similar to the studies performed in cervical cancer, alterations in tumor perfusion parameters

early after the start of chemo-RT for HNC were investigated for prediction of outcome. In one investigation, improved perfusion after 2 weeks of a 7-week definite chemo-RT treatment course correlated with better local control than persistent poor perfusion in advanced HNC.[25] With extensive promising and converging evidence, we still lack a quantitative understanding of the extent of reliability (uncertainty) of these metrics derived from DCE MRI, and such a gap currently hinders our ability to use it for clinical decision making in individualized radiation therapy outside of a trial setting.

DCE imaging for assessment of normal tissue and organ response to radiation dose

Radiation-induced vascular injury in normal tissue and organs can pose a risk for organ function. Radiation can cause vascular damage such as vessel dilation, endothelial cell death and apoptosis, microvessel hemorrhage, and eventually vessel occlusion.[51-55] Vascular damage can subsequently affect organ function, e.g., in the brain, liver and rectum.[56-59] This risk hinders the attempt to increase radiation dose to achieve a better tumor control or even cure the cancer. Early monitoring of vascular response to radiation treatments has the potential to predict the outcome of organ function after therapy, thereby selecting the patient who is resistant to radiation for higher dose, potentially leading to a better chance of tumor local control and better overall therapeutic outcome.

The liver is an organ that is sensitive to radiation. The risk of radiation-induced liver disease (RILD)[60] is a limiting factor for treatment of intra-hepatic cancer with high doses. Symptoms generally occur 2 weeks to 2 months following completion of RT. The clinical outcome ranges from mild, reversible damage to death.[61-63] The pathology of RILD is veno-occlusive disease (VOD), which is characterized by thrombosis within the central veins of the liver producing “post” hepatic congestion.[58] In the past, efforts to develop NTCP models to estimate the likelihood of developing RILD have been based primarily on the planned radiation dose distribution for the normal liver. The ability to predict RILD is improved by including clinical factors.[62,64-69] While these models have permitted the safe delivery of far higher doses of radiation than were previously possible, they also suggest that there is a broad range of individual patient sensitivity that is not reflected by prediction made solely based on the physical dose distribution or general clinical features.

As the basic pathophysiology of RILD is venous occlusion, early assessment of venous perfusion has the potential to select patients with pre-clinical signs of perfusion changes prior to the onset of symptomatic radiation-induced injury. A previous study investigated the portal venous perfusion changes during and after radiation therapy using DCE CT in patients treated with high dose focal radiation therapy.[70,71] It was found that the percentage changes in the regional portal venous perfusion during the course of RT and one month after RT were linearly related to the local doses accumulated up to the times of scanning. In addition to the dose-dependency, the venous perfusion changes one month after RT also correlated with the changes measured after receiving ~ 45Gy during the course of RT, indicating individual sensitivity to radiation. This finding motivated an investigation of the individual portal venous perfusion-dose response function (PVPDRF) - the relationship between the venous perfusion change and the local dose in individual patients.[70] Interestingly, the livers of different patients responded differently to the same radiation dose and/or dose distribution, with critical biologically-corrected doses (/ =2.5) for undetectable portal venous perfusion ranging from 35.2 Gy to 75.6 Gy with a median of 49.3 Gy. Most importantly, the estimated mean portal venous perfusion in normal liver parenchyma correlated with the overall liver function assessed by the clearance time of ICG, suggesting that spatially-resolved portal venous perfusion could be a marker for overall liver function, knowledge of which is required for radiation treatment planning and plan adaptation.

Neurovasculature is also sensitive to radiation. Neurovascular injury might be a part of the dynamic, interactive process of neurotoxicity, and relate to late cognitive dysfunction. Due to the prolonged survival of some patients with brain tumors following treatment with radiation and the advance in MRI technologies, delayed or late micro-hemorrhage in the brain has been observed, and appears to have an incidence higher than anticipated previously.

Effects of dose and dose-volume on neurovascular injury, tissue degeneration (white matter demyelination and necrosis), and cognitive dysfunction are not well understood. Radiation-induced vascular alteration also poses difficulty to differentiate tumor recurrence from radiation necrosis.[56,72] Several investigations attempt to shed light on these questions.[56,57,73] A longitudinal investigation of neurovascular changes as well as cognitive function changes after conformal, whole brain or stereotactic radiation therapy could provide an insight into these questions. A prospective study of DCE MRI for prediction of radiation-induced neurocognitive dysfunction found that cerebral blood volumes and blood-brain barrier (BBB) permeability increase significantly in the high dose regions during RT, followed by a decrease after RT.[57] Changes in both cerebral blood volume and BBB permeability correlated with the doses accumulated at the time of scans at week 3 and 6 during the course of RT and 1 month after RT. The effect of the dose-volume on the vascular volume was also observed. Finally, changes in verbal memory and learning scores 6 months after RT were significantly correlated with changes in cerebral blood volumes of left temporal and frontal lobes and changes in BBB permeability of left frontal lobes during RT, indicating the potential to use early changes in neurovasculature assessed by DCE MRI as a biomarker for late neurocognitive changes. Although other imaging modalities are also able to assess changes in cerebral blood flow and cerebral blood volume after RT,[74,75] DCE and DSC MRI are more suitable for repeated measures as required by a longitudinal study, and also allow assessment of CBV, CBF, and vascular permeability in a single scan that lasts just a few minutes. A further understanding of relationships of delayed micro-bleeding to late neurocognitive function change, to tissue degeneration, to early vascular changes, and to dose and dose-volume could provide guidance on radiation treatment planning and improve quality of life.

DCE MRI for radiation target selection and delineation

As technological dose delivery has changed dramatically, target volume definition based upon CT is increasingly becoming an obvious limiting factor in advanced precision treatment. The role of functional imaging for target volume definition has been discussed by several authors.[1,76] It has been suggested that a tumor target volume could be defined and segmented as multiple biological target sub-volumes, which could be defined based upon multiple functional imaging examinations, each of which could be a prognostic factor for radiation response.[1] Dose sculpting and painting of multiple biological target sub-volumes has been hypothesized.[1,2] For such high precision radiation treatment, it is important to understand the sensitivity and specificity of a functional imaging methodology for localization and delineation of a tumor or sub-volume of tumor, and how the discriminative capacity of these added biomarkers affects treatment planning. However, few studies have been able to address this question. To this regard, there is a scarcity of work that has been done for DCE imaging, with the exception of prostate cancer.

Substantial investigations have been performed using DCE MRI for localization of prostate cancer.[77-80] In early studies, dynamic enhancement patterns and/or the parameters derived from DCE MRI were visually inspected and scored by radiologists, and then compared to pathological diagnoses.[77,78,81] Overall, sensitivity achieved ranged from 74-93% and specificity from 79-96%, depending upon the experience of reading radiologists, imaging acquisition protocol, and the parameters derived from DCE MRI as well as image

processing approaches if used.[77,7882,83] Also, a lower rate of localization of cancer was observed in the transition zone than in the peripheral zone.[78] In some studies, DCE MRI for localization of prostate cancer has been compared to T2-weighted, diffusion, and spectroscopic MRI, and it is often reported that DCE MRI has superior performance,[81] and a combined approach often shows a marginal improvement.[84] A recent study[85] showed the sensitivity (82%) and specificity (89%) of the vascular parameters derived from DCE MRI for localization of prostate cancer in the left lobe, right lobe or bilaterally are similar to that found in choline PET/CT.[86] Interestingly, the same study found that MRSI has a lower sensitivity and specificity, with 55%-68% for sensitivity and 62%-67% for specificity, depending upon spectroscopy pulse sequences and spatial resolution of spectroscopic images.

In order to support delineating prostate gross cancer volume using DCE MRI, further pathological validation has been done by few studies.[85,87] In one study[85] the parameters derived from DCE MRI were not able to detect lesions with a size less than 3 mm and/or composed of less than 30% tumor cells, whereas MRS failed to detect lesions with a size of less than 8 mm and/or containing 50% cancer cells. While comparing with the histological volume in specimens, DCE MRI-defined volumes underestimated the histological volumes, especially in cases where the prostate cancer showed a diffuse tumor growth with a low density of prostate cancer cells. These findings may also depend upon the imaging protocols used in the study.[85] Nevertheless, delineation of prostate cancer for radiation target remains a great challenge. Another recent study, including a small series of 5 patients, attempted to determine the accuracy of prostate gross tumor volume delineated based upon combination of diffusion and DCE MRI by a radiation oncology expert.[87] Of 22 lesions delineated on prostatectomy specimens by a pathologist, five dominate cancers with volume greater than 1 cc, and four other smaller ones with a minimum volume of 0.56 cc were detected by the experienced radiation oncologist based upon MRI with a spatial resolution of $2.5\times2.5\times2.5mm^3$. The gross tumor volumes of the five dominant cancers delineated on MRI covered 44-76% of the pathologically determined tumor volumes, but had 62-174% of the pathologically determined tumor volumes. In addition to errors of image registration, the mis-matched characteristics between diffusion and vascular parameters (in 3 dominant lesions) and negative appearance on MRI (in 1 dominant lesion) contribute to the missed sub-volumes of the tumor delineated by the radiation oncology expert. The investigators suggested use of a 5 mm margin in the gross tumor volume delineated on the MRI to improve the tumor volume coverage. Using this expansion guideline, gross tumor volumes were 2.5-3 times as large as the pathological tumor volumes. Whether this can be accepted or not for radiation target definition is subject to discussion. Finally, development of multi-parameter MRI and automated methods for detection of prostate cancer in the peripheral zone has been attempted.[88-90] Although these tools are in the preliminary stage of development, they have the potential to overcome difficulties in comparison and replication of the results for localization and delineation of prostate cancer reported by previous studies.

Issues related to DCE imaging in Radiation Therapy

Issues related to the utilization of DCE imaging in radiation oncology perhaps depend upon the attempted usage. There are some common issues related to all types of cancer therapy, but others uniquely to radiation therapy. These common issues include standardization of imaging protocols, the pharmacokinetic models, and quantitative metrics derived from the DCE imaging data, quality control/assurance of imaging acquisition, and reproducibility and accuracy of the method as a whole. Currently, there are several national initiatives that aim to address some of these issues. These include the Reference Image Database to Evaluate Response to Therapy (RIDER) project of the National Cancer Institute's Cancer Imaging Program, Quantitative Image Network (QIN) of the National Cancer Institute (https://

wiki.nci.nih.gov/display/CIP/QIN), and Quantitative Imaging Biomarker alliance (QIBA) (http://qibawiki.rsna.org). One of the issues that has been focused on from such initiatives is the physical uncertainty resulting from image acquisition.[91,92] The physical uncertainty of the quantitative metrics derived from DCE imaging can result from image acquisition as well as computation methods,[93] and can be random and systemic (biased). The physical uncertainty needs to be characterized, and thereby to be powered into the clinical trials to assess a given size of biological effects of therapy.[91]

Currently, image acquisition protocols and processing strategies are far from being standardized, which hinders cross comparison of the data from different labs or trials as well as conducting multi-center trials. The reproducibility of the DCE quantitative metrics, which can result from both physical uncertainty and biological uncertainty, determines the ability of a metric to measure therapy response in individual patients. The reproducibility of a metric may also be tumor site specific due to biological variation. A few technical aspects of the issues, such as the measurement of arterial input function due to acquisition parameters as well as its influence on the derived parameters,[94-98] sensitivity of the derived parameters upon quantification software of the pharmacokinetic (PK) model, image quality and acquisition parameters additional to arterial input function,[93] and repeatability of the parameters based upon the PK models or non-PK models in the tumor and normal tissue, have been investigated.[99-102] These efforts are works in progress, and few repeat image data sets are available to the scientific community for analysis.

In addition, lack of standards for image acquisition, parameter quantification methods, and statistical metrics (or methods)[103] makes it difficult to interpret and utilize the limited published information. Uncertainty of image registration among the series of DCE images acquired over a period of time and to the treatment planning CT is also an issue. Although it is not unique for DCE imaging in radiation therapy assessment, misalignment between a pair of images acquired at different time points challenges the validity of voxel-level statistical analysis. Although deformable image registration can achieve better geometric accuracy than rigid body methods, irregularity of the deformable field can propagate into the signal intensity interpolation in the parameter map,[104] and result in more errors in the signal intensities, in severe cases yielding a salt-and-pepper looking image, which is more problematic for a functional or physiological parameter image than a geometric image. In additional to the technical validation issues, the derived parameter has to have sufficient sensitivity and specificity for the clinical problem addressed, e.g. prediction for tumor local control, time to disease survival, or overall survival.

There are further challenges for utilization of DCE imaging in radiation therapy. Radiation treatment and planning need to consider where the tumor is spatially, where the extent or margin of the tumor is, where tumor response is, and where the tumor at risk for failure is, in order to delineate radiation targets and define boost volumes. In the consideration of tumor delineation, it is important to understand how sensitive DCE imaging is to the tumor size and tumor cell density and how specific it may be for distinguishing the tumor from other tissues. It is important to perform pathological validation of DCE imaging for tumor delineation, which has been only pursued in a limited fashion and presents great challenges technically and clinically. Comparing image-derived tumor patterns of failure with the parameter map of DCE imaging could aid in assessing the value of DCE, particularly for organs where a pathological sample is hard to obtain, e.g., in the brain.

In summary, the wealth of information provided by perfusion estimation through dynamic contrast enhanced imaging is providing new insights into prognosis as well as assessment of tumor and normal tissue responses to radiation and combined modality therapies. Such imaging may play a role in treatment modality selection, target definition, and therapy

individualization, although the evidence supporting these roles is still preliminary. To progress from preliminary studies to broad application, a number of validation steps, both technical as well as clinical/pathological, are needed. National efforts at technical validation will support the optimal use of DCE as a biomarker, and ideally early stage clinical trials will expand into broader investigations leading to establishment of this important methodology in routine clinical care.

Acknowledgments

Yue Cao' research is supported in part by NIH P01 CA59827, NCI RO1 CA132834, RO1 NS064973 and R21 CA126137.

References

1. Gregoire V, Haustermans K. Functional image-guided intensity modulated radiation therapy: integration of the tumour microenvironment in treatment planning. Eur J Cancer. 2009; 45(1):459–60. [PubMed: 19775671]
2. Ling CC, Humm J, Larson S, et al. Towards multidimensional radiotherapy (MD-CRT): biological imaging and biological conformality. Int J Radiat Oncol Biol Phys. 2000; 47:551–60. [PubMed: 10837935]
3. Hermans R, Meijerink M, Van den Bogaert W, et al. Tumor perfusion rate determined noninvasively by dynamic computed tomography predicts outcome in head-and-neck cancer after radiotherapy. Int J Radiat Oncol Biol Phys. 2003; 57:1351–6. [PubMed: 14630273]
4. Cao Y, Sundgren PC, Tsien CI, et al. Physiologic and metabolic magnetic resonance imaging in gliomas. J Clin Oncol. 2006; 24:1228–35. [PubMed: 16525177]
5. Law M, Young RJ, Babb JS, et al. Gliomas: predicting time to progression or survival with cerebral blood volume measurements at dynamic susceptibility-weighted contrast-enhanced perfusion MR imaging. Radiology. 2008; 247:490–8. [PubMed: 18349315]
6. Rosen BR, Belliveau JW, Aronen HJ, et al. Susceptibility contrast imaging of cerebral blood volume: human experience. Magn Reson Med. 1991; 22:293–9. discussion 300-3. [PubMed: 1812360]
7. Ewing JR, Knight RA, Nagaraja TN, et al. Patlak plots of Gd-DTPA MRI data yield blood-brain transfer constants concordant with those of 14C-sucrose in areas of blood-brain opening. Magn Reson in Med. 2003; 50:283–292. [PubMed: 12876704]
8. Roberts HC, Roberts TP, Brasch RC, et al. Quantitative measurement of microvascular permeability in human brain tumors achieved using dynamic contrast-enhanced MR imaging: correlation with histologic grade. AJNR Am J Neuroradiol. 2000; 21:891–9. [PubMed: 10815665]
9. Provenzale JM, Wang GR, Brenner T, et al. Comparison of permeability in high-grade and low-grade brain tumors using dynamic susceptibility contrast MR imaging. AJR Am J Roentgenol. 2002; 178:711–6. [PubMed: 11856703]
10. Law M, Yang S, Babb JS, et al. Comparison of cerebral blood volume and vascular permeability from dynamic susceptibility contrast-enhanced perfusion MR imaging with glioma grade. AJNR Am J Neuroradiol. 2004; 25:746–55. [PubMed: 15140713]
11. Aronen HJ, Gazit IE, Louis DN, et al. Cerebral blood volume maps of gliomas: comparison with tumor grade and histologic findings. Radiology. 1994; 191:41–51. [PubMed: 8134596]
12. Sugahara T, Korogi Y, Kochi M, et al. Correlation of MR imaging-determined cerebral blood volume maps with histologic and angiographic determination of vascularity of gliomas. AJR Am J Roentgenol. 1998; 171:1479–86. [PubMed: 9843274]
13. Ostergaard L, Sorensen AG, Kwong KK, et al. High resolution measurement of cerebral blood flow using intravascular tracer bolus passages. Part II: Experimental comparison and preliminary results. Magn Reson Med. 1996; 36:726–36. [PubMed: 8916023]
14. Tofts PS, Brix G, Buckley DL, et al. Estimating kinetic parameters from dynamic contrast-enhanced T(1)- weighted MRI of a diffusable tracer: standardized quantities and symbols. J Magn Reson Imaging. 1999; 10:223–32. [PubMed: 10508281]

15. Cao Y, Nagesh V, Hamstra D, et al. The extent and severity of vascular leakage as evidence of tumor aggressiveness in high-grade gliomas. Cancer Res. 2006; 66:8912–7. [PubMed: 16951209]
16. Cao Y, Tsien CI, Nagesh V, et al. Clinical investigation survival prediction in high-grade gliomas by MRI perfusion before and during early stage of RT. Int J Radiat Oncol Biol Phys. 2006; 64:876–85. [PubMed: 16298499]
17. Knopp EA, Cha S, Johnson G, et al. Glial neoplasms: dynamic contrast-enhanced T2*-weighted MR imaging. Radiology. 1999; 211:791–8. [PubMed: 10352608]
18. Lev MH, Ozsunar Y, Henson JW, et al. Glial tumor grading and outcome prediction using dynamic spin-echo MR susceptibility mapping compared with conventional contrast-enhanced MR: confounding effect of elevated rCBV of oligodendrogliomas [corrected]. AJNR Am J Neuroradiol. 2004; 25:214–21. [PubMed: 14970020]
19. Linderholm B, Grankvist K, Wilking N, et al. Correlation of vascular endothelial growth factor content with recurrences, survival, and first relapse site in primary node-positive breast carcinoma after adjuvant treatment. J Clin Oncol. 2000; 18:1423–31. [PubMed: 10735889]
20. Schneider BP, Miller KD. Angiogenesis of breast cancer. J Clin Oncol. 2005; 23:1782–90. [PubMed: 15755986]
21. Brizel DM, Dodge RK, Clough RW, et al. Oxygenation of head and neck cancer: changes during radiotherapy and impact on treatment outcome. Radiother Oncol. 1999; 53:113–7. [PubMed: 10665787]
22. Stadler P, Becker A, Feldmann HJ, et al. Influence of the hypoxic subvolume on the survival of patients with head and neck cancer. Int J Radiat Oncol Biol Phys. 1999; 44:749–54. [PubMed: 10386631]
23. Nordsmark M, Overgaard J. A confirmatory prognostic study on oxygenation status and loco-regional control in advanced head and neck squamous cell carcinoma treated by radiation therapy. Radiother Oncol. 2000; 57:39–43. [PubMed: 11033187]
24. Nordsmark M, Overgaard M, Overgaard J. Pretreatment oxygenation predicts radiation response in advanced squamous cell carcinoma of the head and neck. Radiother Oncol. 1996; 41:31–9. [PubMed: 8961365]
25. Cao Y, Popovtzer A, Li D, et al. Early prediction of outcome in advanced head-and-neck cancer based on tumor blood volume alterations during therapy: a prospective study. Int J Radiat Oncol Biol Phys. 2008; 72:1287–90. [PubMed: 19028268]
26. Lehtio K, Eskola O, Viljanen T, et al. Imaging perfusion and hypoxia with PET to predict radiotherapy response in head-and-neck cancer. Int J Radiat Oncol Biol Phys. 2004; 59:971–82. [PubMed: 15234030]
27. Brandes AA, Franceschi E, Tosoni A, et al. MGMT promoter methylation status can predict the incidence and outcome of pseudoprogression after concomitant radiochemotherapy in newly diagnosed glioblastoma patients. J Clin Oncol. 2008; 26:2192–7. [PubMed: 18445844]
28. Kumar B, Cordell KG, Lee JS, et al. EGFR, p16, HPV Titer, Bcl-xL and p53, sex, and smoking as indicators of response to therapy and survival in oropharyngeal cancer. J Clin Oncol. 2008; 26:3128–37. [PubMed: 18474878]
29. Worden FP, Kumar B, Lee JS, et al. Chemoselection as a strategy for organ preservation in advanced oropharynx cancer: response and survival positively associated with HPV16 copy number. J Clin Oncol. 2008; 26:3138–46. [PubMed: 18474879]
30. Hafkamp HC, Manni JJ, Haesevoets A, et al. Marked differences in survival rate between smokers and nonsmokers with HPV 16-associated tonsillar carcinomas. Int J Cancer. 2008; 122:2656–64. [PubMed: 18360824]
31. Fakhry C, Westra WH, Li S, et al. Improved survival of patients with human papillomavirus-positive head and neck squamous cell carcinoma in a prospective clinical trial. J Natl Cancer Inst. 2008; 100:261–9. [PubMed: 18270337]
32. Chi AS, Sorensen AG, Jain RK, et al. Angiogenesis as a therapeutic target in malignant gliomas. Oncologist. 2009; 14:621–36. [PubMed: 19487335]
33. Sorensen AG, Batchelor TT, Zhang WT, et al. A “vascular normalization index” as potential mechanistic biomarker to predict survival after a single dose of cediranib in recurrent glioblastoma patients. Cancer Res. 2009; 69:5296–300. [PubMed: 19549889]

34. Galban CJ, Chenevert TL, Meyer CR, et al. The parametric response map is an imaging biomarker for early cancer treatment outcome. Nat Med. 2009; 15:572–6. [PubMed: 19377487]
35. Tsien C, Galban CJ, Chenevert TL, et al. Parametric response map as an imaging biomarker to distinguish progression from pseudoprogression in high-grade glioma. J Clin Oncol. 2010; 28:2293–9. [PubMed: 20368564]
36. Essig M, Waschkies M, Wenz F, et al. Assessment of brain metastases with dynamic susceptibility-weighted contrast-enhanced MR imaging: initial results. Radiology. 2003; 228:193–9. [PubMed: 12832582]
37. Weber MA, Thilmann C, Lichy MP, et al. Assessment of irradiated brain metastases by means of arterial spin-labeling and dynamic susceptibility-weighted contrast-enhanced perfusion MRI: initial results. Invest Radiol. 2004; 39:277–87. [PubMed: 15087722]
38. Huber PE, Hawighorst H, Fuss M, et al. Transient enlargement of contrast uptake on MRI after linear accelerator (linac) stereotactic radiosurgery for brain metastases. Int J Radiat Oncol Biol Phys. 2001; 49:1339–49. [PubMed: 11286842]
39. Loncaster JA, Carrington BM, Sykes JR, et al. Prediction of radiotherapy outcome using dynamic contrast enhanced MRI of carcinoma of the cervix. Int J Radiat Oncol Biol Phys. 2002; 54:759–67. [PubMed: 12377328]
40. Mayr NA, Yuh WT, Magnotta VA, et al. Tumor perfusion studies using fast magnetic resonance imaging technique in advanced cervical cancer: a new noninvasive predictive assay. Int J Radiat Oncol Biol Phys. 1996; 36:623–33. [PubMed: 8948347]
41. Mayr NA, Yuh WT, Arnholt JC, et al. Pixel analysis of MR perfusion imaging in predicting radiation therapy outcome in cervical cancer. J Magn Reson Imaging. 2000; 12:1027–33. [PubMed: 11105046]
42. Yamashita Y, Baba T, Baba Y, et al. Dynamic contrast-enhanced MR imaging of uterine cervical cancer: pharmacokinetic analysis with histopathologic correlation and its importance in predicting the outcome of radiation therapy. Radiology. 2000; 216:803–9. [PubMed: 10966715]
43. Mayr NA, Wang JZ, Zhang D, et al. Longitudinal changes in tumor perfusion pattern during the radiation therapy course and its clinical impact in cervical cancer. Int J Radiat Oncol Biol Phys. 77:502–8. [PubMed: 19775824]
44. Hermans R, Lambin P, Van den Bogaert W, et al. Non-invasive tumour perfusion measurement by dynamic CT: preliminary results. Radiother Oncol. 1997; 44:159–62. [PubMed: 9288844]
45. Hoskin PJ, Saunders MI, Goodchild K, et al. Dynamic contrast enhanced magnetic resonance scanning as a predictor of response to accelerated radiotherapy for advanced head and neck cancer. Br J Radiol. 1999; 72:1093–8. [PubMed: 10700827]
46. Gandhi D, Chepeha DB, Miller T, et al. Correlation between initial and early follow-up CT perfusion parameters with endoscopic tumor response in patients with advanced squamous cell carcinomas of the oropharynx treated with organ-preservation therapy. AJNR Am J Neuroradiol. 2006; 27:101–6. [PubMed: 16418366]
47. Brun E, Kjellen E, Tennvall J, et al. FDG PET studies during treatment: prediction of therapy outcome in head and neck squamous cell carcinoma. Head Neck. 2002; 24:127–35. [PubMed: 11891942]
48. Zima A, Carlos R, Gandhi D, et al. Can pretreatment CT perfusion predict response of advanced squamous cell carcinoma of the upper aerodigestive tract treated with induction chemotherapy? AJNR Am J Neuroradiol. 2007; 28:328–34. [PubMed: 17297007]
49. Thorwarth D, Eschmann SM, Scheiderbauer J, et al. Kinetic analysis of dynamic 18F-fluoromisonidazole PET correlates with radiation treatment outcome in head-and-neck cancer. BMC Cancer. 2005; 5:152. [PubMed: 16321146]
50. Jansen JF, Schoder H, Lee NY, et al. Noninvasive assessment of tumor microenvironment using dynamic contrast-enhanced magnetic resonance imaging and 18F-fluoromisonidazole positron emission tomography imaging in neck nodal metastases. Int J Radiat Oncol Biol Phys. 2010; 77:1403–10. [PubMed: 19906496]
51. Pena LA, Fuks Z, Kolesnick RN. Radiation-induced apoptosis of endothelial cells in the murine central nervous system: protection by fibroblast growth factor and sphingomyelinase deficiency. Cancer Res. 2000; 60:321–7. [PubMed: 10667583]

52. Ljubimova NV, Levitman MK, Plotnikova ED, et al. Endothelial cell population dynamics in rat brain after local irradiation. Br J Radiol. 1991; 64:934–40. [PubMed: 1954536]
53. Santana P, Pena LA, Haimovitz-Friedman A, et al. Acid sphingomyelinase-deficient human lymphoblasts and mice are defective in radiation-induced apoptosis. Cell. 1996; 86:189–99. [PubMed: 8706124]
54. Brown WR, Thore CR, Moody DM, et al. Vascular damage after fractionated whole-brain irradiation in rats. Radiat Res. 2005; 164:662–8. [PubMed: 16238444]
55. Cao Y, Tsien CI, Shen Z, et al. Use of magnetic resonance imaging to assess blood-brain/blood-glioma barrier opening during conformal radiotherapy. J Clin Oncol. 2005; 23:4127–36. [PubMed: 15961760]
56. Sundgren PC, Cao Y. Brain irradiation: effects on normal brain parenchyma and radiation injury. Neuroimaging Clin N Am. 2009; 19:657–68. [PubMed: 19959011]
57. Cao Y, Tsien CI, Sundgren P, et al. DCE MRI as a Biomarker for Prediction of Radiation-Induced Neurocognitive Dysfunction. Clinical Cancer Research. 2009; 15:1747–54. [PubMed: 19223506]
58. Lawrence TS, Robertson JM, Anscher MS, et al. Hepatic toxicity resulting from cancer treatment. Int J Radiat Oncol Biol Phys. 1995; 31:1237–48. [PubMed: 7713785]
59. Michalski JM, Gay H, Jackson A, et al. Radiation dose-volume effects in radiation-induced rectal injury. Int J Radiat Oncol Biol Phys. 76:S123–9. [PubMed: 20171506]
60. Emami B, Lyman J, Brown A, et al. Tolerance of normal tissue to therapeutic irradiation. Int J Radiat Oncol Biol Phys. 1991; 21:109–22. [PubMed: 2032882]
61. Lawrence TS, Davis MA, Maybaum J, et al. The potential superiority of bromodeoxyuridine to iododeoxyuridine as a radiation sensitizer in the treatment of colorectal cancer. Cancer Res. 1992; 52:3698–704. [PubMed: 1617642]
62. Russell AH, Clyde C, Wasserman TH, et al. Accelerated hyperfractionated hepatic irradiation in the management of patients with liver metastases: results of the RTOG dose escalating protocol. Int J Radiat Oncol Biol Phys. 1993; 27:117–23. [PubMed: 8365932]
63. Schacter L, Crum E, Spitzer T, et al. Fatal radiation hepatitis: a case report and review of the literature. Gynecol Oncol. 1986; 24:373–80. [PubMed: 3721310]
64. Ingold DK, Reed GB, Kaplan HS, et al. Radiation Hepatitis. Am J Roentgenol. 1965; 93:200–208.
65. Jackson A, Ten Haken RK, Robertson JM, et al. Analysis of clinical complication data for radiation hepatitis using a parallel architecture model. Int J Radiat Oncol Biol Phys. 1995; 31:883–91. [PubMed: 7860402]
66. Dawson LA, Normolle D, Balter JM, et al. Analysis of radiation-induced liver disease using the Lyman NTCP model. Int J Radiat Oncol Biol Phys. 2002; 53:810–21. [PubMed: 12095546]
67. Ten Haken RK, Martel MK, Kessler ML, et al. Use of Veff and iso-NTCP in the implementation of dose escalation protocols. Int J Radiat Oncol Biol Phys. 1993; 27:689–95. [PubMed: 8226166]
68. Poussin-Rosillo H, Nisce LZ, D'Angio GJ. Hepatic radiation tolerance in Hodgkin's disease patients. Radiology. 1976; 121:461–4. [PubMed: 981628]
69. Austin-Seymour MM, Chen GT, Castro JR, et al. Dose volume histogram analysis of liver radiation tolerance. Int J Radiat Oncol Biol Phys. 1986; 12:31–5. [PubMed: 3080390]
70. Cao Y, Pan C, Balter JM, et al. Liver function after irradiation based on computed tomographic portal vein perfusion imaging. Int J Radiat Oncol Biol Phys. 2008; 70:154–60. [PubMed: 17855011]
71. Cao Y, Platt JF, Francis IR, et al. The prediction of radiation-induced liver dysfunction using a local dose and regional venous perfusion model. Med Phys. 2007; 34:604–12. [PubMed: 17388178]
72. Jain R, Scarpace L, Ellika S, et al. First-pass perfusion computed tomography: initial experience in differentiating recurrent brain tumors from radiation effects and radiation necrosis. Neurosurgery. 2007; 61:778–86. discussion 786-7. [PubMed: 17986939]
73. Lee MC, Cha S, Chang SM, et al. Dynamic susceptibility contrast perfusion imaging of radiation effects in normal-appearing brain tissue: changes in the first-pass and recirculation phases. J Magn Reson Imaging. 2005; 21:683–93. [PubMed: 15906330]

74. Taki S, Higashi K, Oguchi M, et al. Changes in regional cerebral blood flow in irradiated regions and normal brain after stereotactic radiosurgery. Ann Nucl Med. 2002; 16:273–7. [PubMed: 12126097]
75. Hahn CA, Zhou SM, Raynor R, et al. Dose-dependent effects of radiation therapy on cerebral blood flow, metabolism, and neurocognitive dysfunction. Int J Radiat Oncol Biol Phys. 2009; 73:1082–7. [PubMed: 18755558]
76. Grosu AL, Nestle U, Weber WA. How to use functional imaging information for radiotherapy planning. Eur J Cancer. 2009; 45(1):461–3. [PubMed: 19775672]
77. Jager GJ, Ruijter ET, van de Kaa CA, et al. Dynamic TurboFLASH subtraction technique for contrast-enhanced MR imaging of the prostate: correlation with histopathologic results. Radiology. 1997; 203:645–52. [PubMed: 9169683]
78. Ogura K, Maekawa S, Okubo K, et al. Dynamic endorectal magnetic resonance imaging for local staging and detection of neurovascular bundle involvement of prostate cancer: correlation with histopathologic results. Urology. 2001; 57:721–6. [PubMed: 11306390]
79. Noworolski SM, Henry RG, Vigneron DB, et al. Dynamic contrast-enhanced MRI in normal and abnormal prostate tissues as defined by biopsy, MRI, and 3D MRSI. Magn Reson Med. 2005; 53:249–55. [PubMed: 15678552]
80. Kiessling F, Lichy M, Grobholz R, et al. Simple models improve the discrimination of prostate cancers from the peripheral gland by T1-weighted dynamic MRI. Eur Radiol. 2004; 14:1793–801. [PubMed: 15232714]
81. Futterer JJ, Heijmink SW, Scheenen TW, et al. Prostate cancer localization with dynamic contrast-enhanced MR imaging and proton MR spectroscopic imaging. Radiology. 2006; 241:449–58. [PubMed: 16966484]
82. Hara N, Okuizumi M, Koike H, et al. Dynamic contrast-enhanced magnetic resonance imaging (DCE-MRI) is a useful modality for the precise detection and staging of early prostate cancer. Prostate. 2005; 62:140–7. [PubMed: 15389803]
83. Puech P, Potiron E, Lemaitre L, et al. Dynamic contrast-enhanced-magnetic resonance imaging evaluation of intraprostatic prostate cancer: correlation with radical prostatectomy specimens. Urology. 2009; 74:1094–9. [PubMed: 19773038]
84. Kozlowski P, Chang SD, Jones EC, et al. Combined diffusion-weighted and dynamic contrast-enhanced MRI for prostate cancer diagnosis--correlation with biopsy and histopathology. J Magn Reson Imaging. 2006; 24:108–13. [PubMed: 16767709]
85. Schmuecking M, Boltze C, Geyer H, et al. Dynamic MRI and CAD vs. choline MRS: where is the detection level for a lesion characterisation in prostate cancer? Int J Radiat Biol. 2009; 85:814–24. [PubMed: 19701842]
86. Reske SN, Blumstein NM, Neumaier B, et al. Imaging prostate cancer with 11C-choline PET/CT. J Nucl Med. 2006; 47:1249–54. [PubMed: 16883001]
87. Groenendaal G, Moman MR, Korporaal JG, et al. Validation of functional imaging with pathology for tumor delineation in the prostate. Radiother Oncol. 2010; 94:145–50. [PubMed: 20116116]
88. Vos PC, Hambrock T, Hulsbergen-van de Kaa CA, et al. Computerized analysis of prostate lesions in the peripheral zone using dynamic contrast enhanced MRI. Med Phys. 2008; 35:888–99. [PubMed: 18404925]
89. Langer DL, van der Kwast TH, Evans AJ, et al. Prostate cancer detection with multi-parametric MRI: logistic regression analysis of quantitative T2, diffusion-weighted imaging, and dynamic contrast-enhanced MRI. J Magn Reson Imaging. 2009; 30:327–34. [PubMed: 19629981]
90. Puech P, Betrouni N, Makni N, et al. Computer-assisted diagnosis of prostate cancer using DCE-MRI data: design, implementation and preliminary results. Int J Comput Assist Radiol Surg. 2009; 4:1–10. [PubMed: 20033597]
91. Clarke LP, Croft BS, Nordstrom R, et al. Quantitative imaging for evaluation of response to cancer therapy. Transl Oncol. 2009; 2:195–7. [PubMed: 19956378]
92. Jackson EF, Barboriak DP, Bidaut LM, et al. Magnetic resonance assessment of response to therapy: tumor change measurement, truth data and error sources. Transl Oncol. 2009; 2:211–5. [PubMed: 19956380]

93. Cao Y, Li D, Shen Z, et al. Sensitivity of Quantitative Metrics Derived from DCE MRI and a Pharmacokinetic Model to Image Quality and Acquisition Parameters. Academic Radiology. 2010; 17:468–478. [PubMed: 20207317]
94. Henderson E, Rutt BK, Lee TY. Temporal sampling requirements for the tracer kinetics modeling of breast disease. Magn Reson Imaging. 1998; 16:1057–73. [PubMed: 9839990]
95. Calamante F, Gadian DG, Connelly A. Delay and dispersion effects in dynamic susceptibility contrast MRI: simulations using singular value decomposition. Magn Reson Med. 2000; 44:466–73. [PubMed: 10975900]
96. Cheng HL. Investigation and optimization of parameter accuracy in dynamic contrast-enhanced MRI. J Magn Reson Imaging. 2008; 28:736–43. [PubMed: 18777534]
97. Peeters F, Annet L, Hermoye L, et al. Inflow correction of hepatic perfusion measurements using T1-weighted, fast gradient-echo, contrast-enhanced MRI. Magn Reson Med. 2004; 51:710–7. [PubMed: 15065243]
98. Singh A, Rathore RK, Haris M, et al. Improved bolus arrival time and arterial input function estimation for tracer kinetic analysis in DCE-MRI. J Magn Reson Imaging. 2009; 29:166–76. [PubMed: 19097111]
99. Jackson A, Jayson GC, Li KL, et al. Reproducibility of quantitative dynamic contrast-enhanced MRI in newly presenting glioma. Br J Radiol. 2003; 76:153–62. [PubMed: 12684231]
100. Galbraith SM, Lodge MA, Taylor NJ, et al. Reproducibility of dynamic contrast-enhanced MRI in human muscle and tumours: comparison of quantitative and semi-quantitative analysis. NMR Biomed. 2002; 15:132–42. [PubMed: 11870909]
101. Padhani AR, Hayes C, Landau S, et al. Reproducibility of quantitative dynamic MRI of normal human tissues. NMR Biomed. 2002; 15:143–53. [PubMed: 11870910]
102. Yang C, Karczmar GS, Medved M, et al. Reproducibility assessment of a multiple reference tissue method for quantitative dynamic contrast enhanced-MRI analysis. Magn Reson Med. 2009; 61:851–9. [PubMed: 19185002]
103. Barnhart HX, Barboriak DP. Applications of the repeatability of quantitative imaging biomarkers: a review of statistical analysis of repeat data sets. Transl Oncol. 2009; 2:231–5. [PubMed: 19956383]
104. Yin LS, Tang L, Hamarneh G, et al. Complexity and accuracy of image registration methods in SPECT-guided radiation therapy. Phys Med Biol. 55:237–46. [PubMed: 20009199]

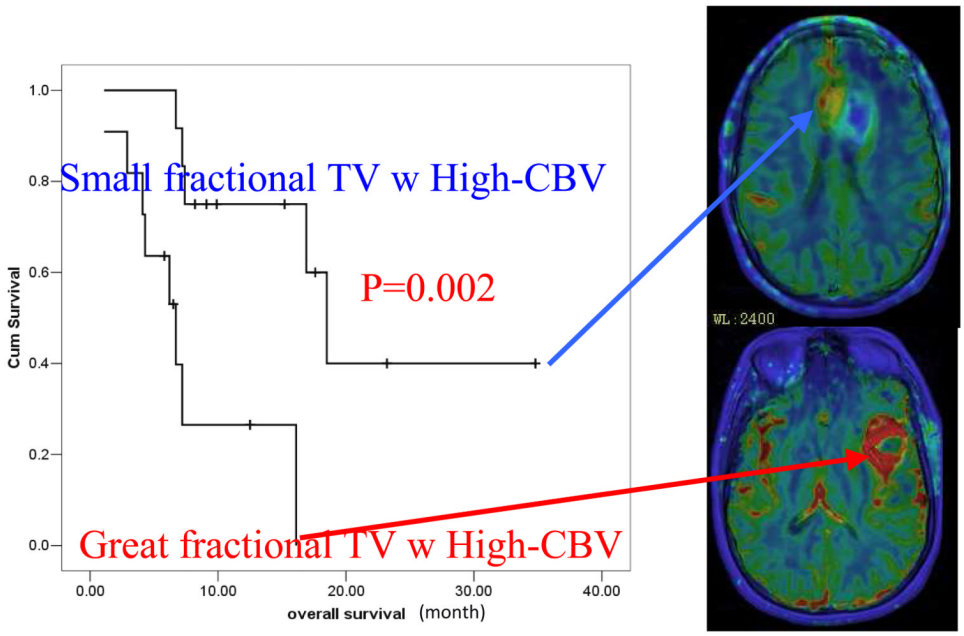

Figure 1.
Survival is significantly worse for the patients who have high-grade gliomas with great fractional tumor volumes with high CBV pre RT than those with small fractional tumor volumes with high CBV.

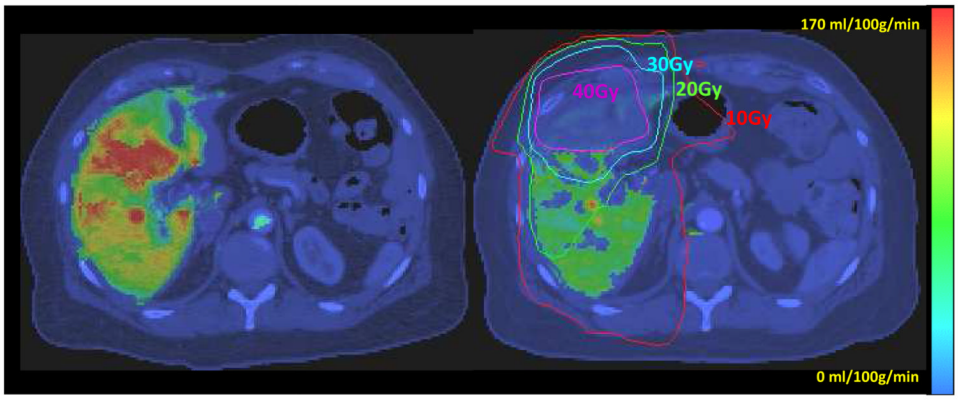

Figure 2.

Portal vein perfusion maps prior to RT (left)_and after the tumor received 46.5 Gy (right) color-coded and overlaid on the liver axial CT. Note that the substantial reduction in venous perfusion in the region received more than 40 Gy (right). Both images were windowed identically. (Figure 3 in Cao et al, Med. Phys. 34(2):604-612, 2007. pending on copy right permission from the journal)

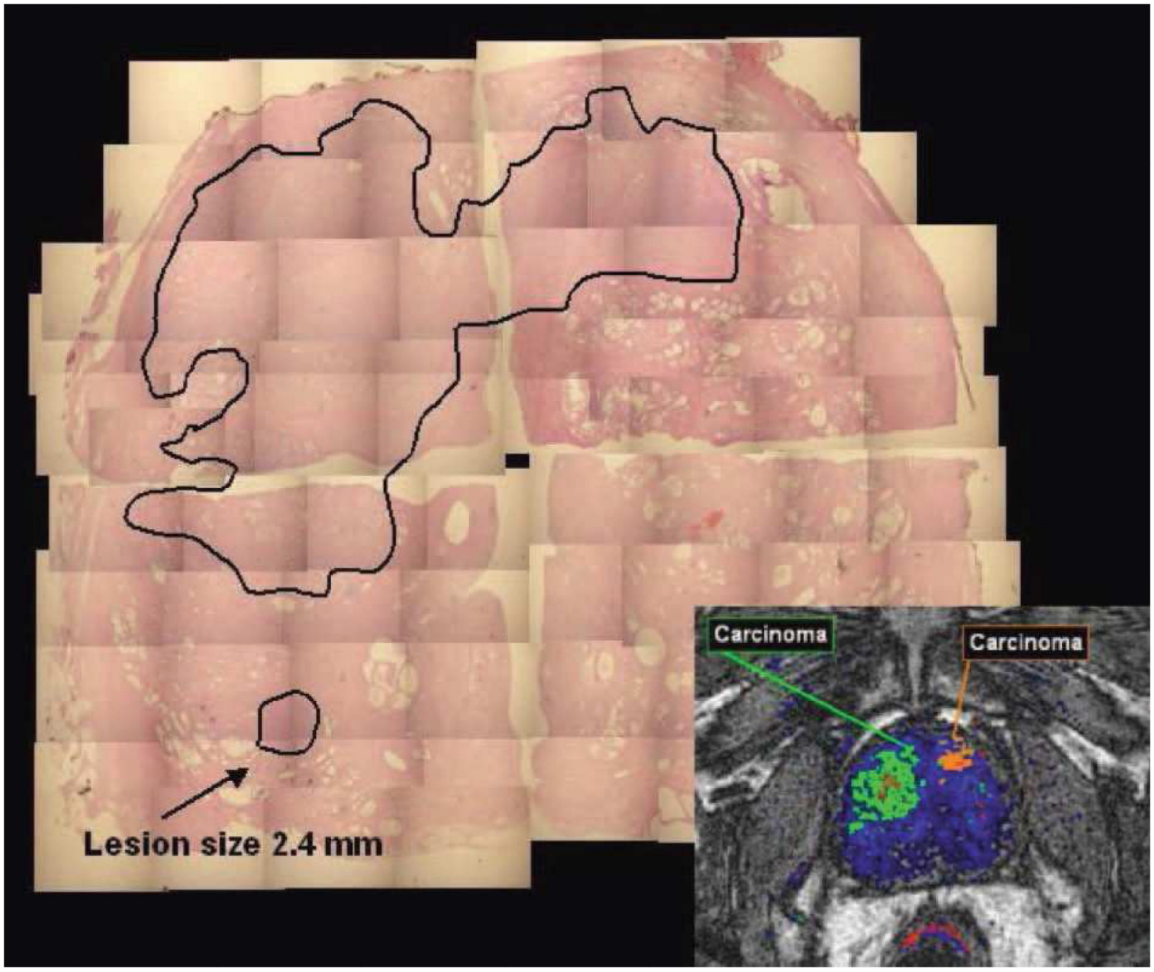

Figure 3.

Two large lesions were detected by DCE-MRI. The lesion in the dorsal part of the right lobe of the prostate being smaller than 3 mm and containing less than 30% of cancer cells was not detected by DCE-MRI. (Figure 6 in SCHMUECKING et al, Int. J. Radiat. Biol., Vol. 85, No. 9, September 2009, pp. 814–824, pending on copy right permission from the journal)